NASA DEVELOP National Program
California – JPL

Fall 2024

Santa Clarita Valley Ecological Conservation

Identifying Oak Woodland Infested with the Goldspotted Oak Borer in the Santa Clarita Valley Using Earth Observations

DEVELOP Technical Report
November 22nd, 2024

Madison Elowitt, Analytical Mechanics & Associates (Project Lead)
Justine Pendergraft, Analytical Mechanics & Associates
Simon Ng, Analytical Mechanics & Associates
Nathalie Lai, Analytical Mechanics & Associates

Advisors:
Daniel Jensen, NASA Jet Propulsion Laboratory, California Institute of Technology (Science Advisor)
Latha Baskaran, NASA Jet Propulsion Laboratory, California Institute of Technology (Science Advisor)
Zoe Pierrat, NASA Jet Propulsion Laboratory, California Institute of Technology (Science Advisor)
Benjamin Holt, NASA Jet Propulsion Laboratory, California Institute of Technology (Science Advisor)

Lead:
Michael Pazmino (California – JPL)

1. Abstract

The recent arrival of the invasive Goldspotted Oak Borer (GSOB; *Agrilus auroguttatus*) into Newhall Pass, California threatens oak woodlands in the Santa Clarita Valley and risks spreading into the Santa Monica Mountains. Without early intervention, previous GSOB infestations have led to widespread oak mortality. Currently, the Mountains Recreation and Conservation Authority and the Resource Conservation District of the Santa Monica Mountains, our two partners, employ ground surveys for GSOB detection and decision-making processes. Comprehensive surveys are constrained by rugged terrain and reliance of visible symptoms, which typically develop several years after the initial infestation, to identify infested trees. This study evaluated the feasibility of using Earth observations—specifically, the Airborne Visible InfraRed Imaging Spectrometer-3 (AVIRIS-3), Landsat 8 Operational Land Imager (OLI) & Thermal Infrared Sensor (TIRS), Landsat 9 OLI-2 & TIRS-2, and Sentinel-2 Multispectral Instrument (MSI) to assess the extent of GSOB infestations in the Santa Clarita Valley, identify regions susceptible to future spread, and examine historical landcover changes linked to GSOB activity. We demonstrated the capability of low altitude 2.9 m-resolution AVIRIS-3 hyperspectral imagery to accurately identify infested oaks (74.7%) within the study area. We further identified areas in Los Angeles and Ventura Counties at high risk for future infestation and illustrated that the 10m-resolution Sentinel-2 NDVI time series did not show the historical spread of infestation. The tools and models developed in this project offer valuable insights for future decision-making aimed at early detection and mitigation of the GSOB spread to ultimately protect oak ecosystems.

Key Terms:
Woodboring beetle, early detection, hyperspectral imagery, AVIRIS-3, risk assessment, landcover change, NDVI, Southern California

2. Introduction

As a keystone genus, oak trees provide essential ecosystem services to Southern California. These trees not only provide a vital food source but also create the habitats, shelters, and microclimatic conditions across various forest layers necessary to sustain biodiversity (Sánchez-González et al., 2015). Over the past two decades, the introduction of the Goldspotted Oak Borer (GSOB; *Agrilus auroguttatus*), an invasive species native to Arizona, has presented a novel threat to oak woodlands. The GSOB is likely transported to new areas via firewood distribution (Coleman & Seybold, 2016), and their larvae tunnel into a tree's cambium to directly feed off its nutrients and water supply, leading to crown thinning and eventual mortality (Haavik et al., 2015). Oak decline from this kind of insect infestation can be slow, with several years between initial infestation and visible symptoms (Corella et al., 2020).

San Diego County first documented the GSOB in 2004 and observed dramatic oak mortality as a result (Coleman & Seybold, 2011). Since then, the GSOB has migrated north through Orange, Riverside, and San Bernadino counties, specifically preying on coast live oak (*Quercus agrifolia*), canyon live oak (*Q. chrysolepis*), and California black oak (*Q. kelloggii*; Coleman et al., 2011). In July 2023, the GSOB was identified on iNaturalist in Newhall Pass, the southern entrance to the Santa Clarita Valley. Because the GSOB infestations take several years to intensify and show clear symptoms (Corella et al., 2020), it is likely that the GSOB migrated to Newhall Pass in the years prior to 2023. In light of this and the risk of the GSOB spreading to the Santa Monica Mountains—home to approximately 600,000 coast live oaks (Mountains Recreation and Conservation Authority, 2024)—the Los Angeles County Board of Supervisors passed a motion in May 2024 to investigate the impact of declaring this infestation a state of emergency, a designation that would allocate resources for detection and prevention efforts (Los Angeles County Board of Supervisors, 2024).

To respond to the growing potential for widespread harm to Southern California's oak woodlands, this project assembled a coalition of stakeholders with diverse expertise and ongoing research. Key collaborators included the Mountains Recreation and Conservation Authority (MRCA); the Resource Conservation District of the Santa Monica Mountains (RCDSMM); the University of California Division of Agriculture and Natural Resources; the California Department of Forestry and Fire Protection (CAL FIRE) Forest Entomology and

Pathology Program; California State University, Northridge; Lewis & Clark College; and the United States Forest Service, Southern California Shared Service Area. Our primary end users were the MRCA and the RCDSMM, both of which manage expansive oak woodlands where the GSOB detection, mitigation, and protection efforts are most urgent.

The MRCA oversees parklands, including areas with known GSOB infestations at Newhall Pass (Figure 1). Meanwhile, the RCDSMM manages the Santa Monica Mountains, which, though in close proximity to Newhall Pass, has not yet detected the GSOB as of October 2024. Both organizations are committed to preserving and managing natural areas in the Los Angeles region through research, conservation action, and community education (MRCA, n.d.; RCDSMM, n.d.).

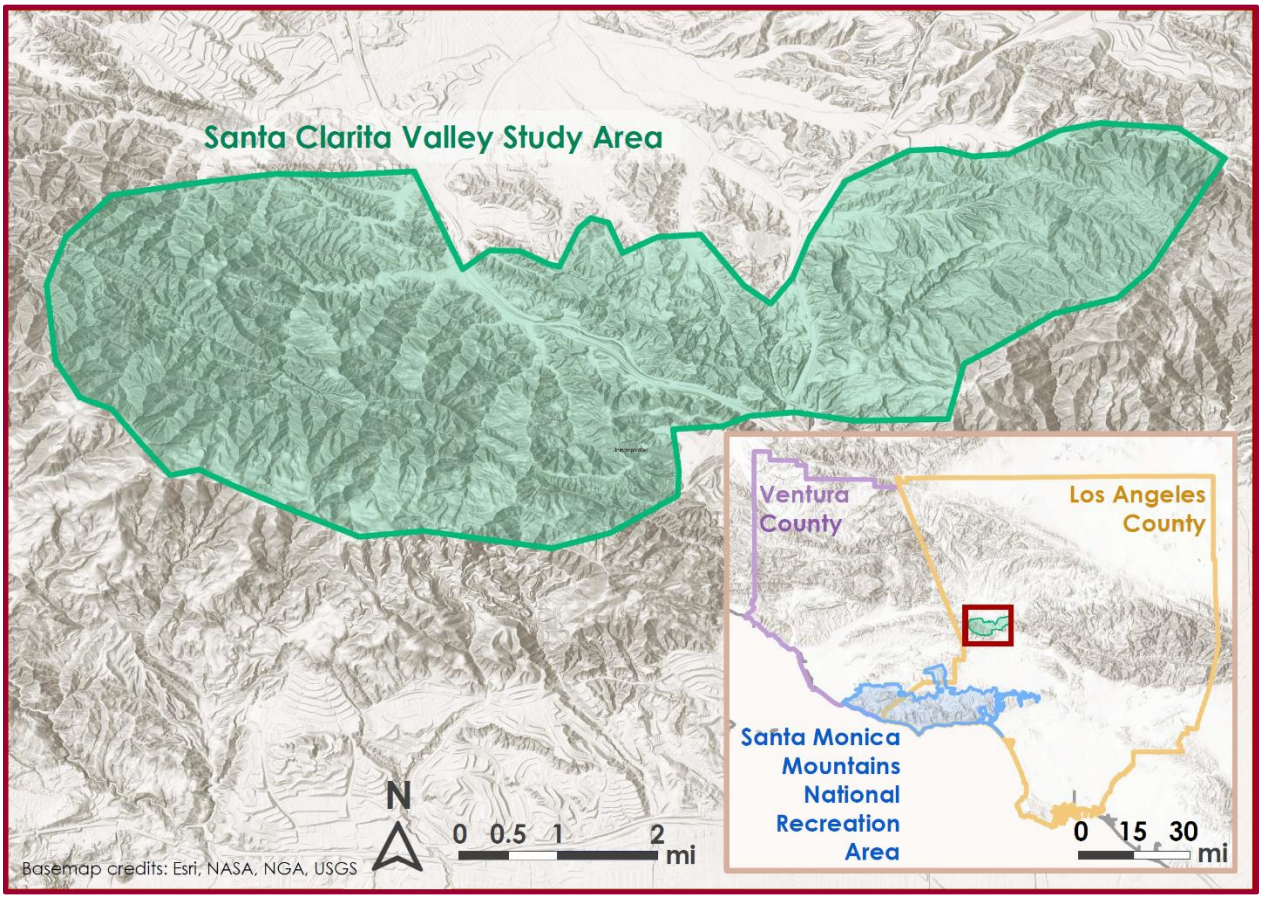

Figure 1. Map of Santa Clarita Valley study area within the broader context of the Santa Monica Mountains National Recreation Area and Los Angeles and Ventura Counties in California.

Currently, the MRCA relies on ground surveys to identify infested trees. However, these surveys are costly, time-consuming, and spatially limited to accessible areas near trails and roads. As a result, scaling these efforts across the rugged oak woodlands of the Santa Clarita Valley presents a significant challenge. Furthermore, the time lag between the initial infestation and the appearance of visible symptoms hinders early detection, as the surveys depend on visual indicators that only become apparent years after the infestation begins.

Previous studies demonstrate the efficacy of utilizing remote sensing to survey forests infested with beetles at larger spatial scales (Senf et al., 2017). In particular, hyperspectral imagery, which captures hundreds of wavelengths, has made early detection more attainable when such data is available and eliminates the reliance on visual symptoms, such as canopy thinning or foliage color changes, as classification criteria. By leveraging the wide range of wavelengths, previous studies have demonstrated the ability to associate early non-visible physiological changes with distinct spectral signatures (Lawrence & Labus, 2003; Gao et al., 2022; Foster et

al., 2017). Hyperspectral data can be combined with machine learning models, like Random Forest (RF) or Support Vector Machines (SVM), to classify tree health based on these unique spectral signatures. Machine learning models are trained with field-collected ground-truth points of infested and non-infested trees (Fassnacht et al., 2014, Gao et al., 2022, Galvan et al., 2023). Ultimately, a good model accurately classifies the infestation status of each tree in the forest so that land managers can identify, prioritize, and address infested areas without the need for extensive ground surveys. The MRCA was interested in incorporating remote sensing methodologies as an alternative tool to complete comprehensive and efficient landscape-scale GSOB surveys and to detect infestations at early stages.

Our project's first goal was to explore the feasibility of tailoring hyperspectral remote sensing methods to observe foliage conditions of oaks in the Santa Clarita Valley to identify and monitor damage from the GSOB threat. In response, we developed a machine learning classification model that infers likely-infested oak trees using field survey data and hyperspectral aerial imagery collected in July 2024 from the Airborne Visible and InfraRed Imaging Spectrometer-3 (AVIRIS-3), the most recent hyperspectral, high-resolution data available. We trained and validated our model based on ground truth data collected by the MRCA and California State University, Northridge collaborators. Our second goal was to produce a risk assessment map that identifies areas within Los Angeles and Ventura Counties at high risk for GSOB infestation. In addition to ancillary datasets that modeled different risks and susceptibility factors, we utilized Landsat 8/9 Thermal Infrared Sensor (TIRS) land surface temperature data from July through October of 2024 to include the impact of heat stress on trees. Our third goal was to investigate the GSOB's initial infestation of the Santa Clarita Valley, which could be associated with seasonal and cumulative changes in oak tree health. Therefore, we conducted a monthly NDVI landcover change analysis using Sentinel-2 datasets between May and September of each year over 2018 and 2024. With these end products and a greater understanding of hyperspectral remote sensing applications to oak woodlands, the MRCA will be able to find, treat, and mitigate the spread of the GSOB within the Santa Clarita Valley, while the RCDSMM will be able to easily detect early migration of the GSOB into the Santa Monica Mountains.

3. Methodology

3.1 Data Acquisition

3.1.1 Infested Oak Classification Map

We downloaded AVIRIS-3 hyperspectral, orthorectified, surface reflectance imagery (285 spectral bands, 380 – 2500 nm with 7.4 nm sampling, Table A1) flown on a B200 Aircraft on July 19, 2024 through the AVIRIS-3 Data Portal (Table C1). The data was originally obtained on a piggyback flight for a pre-planned AVIRIS mission and has a high spatial resolution (2.9 m) which enables tree-level analysis in this project. The flight also occurred recently, giving us up-to-date data so that we can make the best predictions for the current beetle infestation. Hyperspectral sensors return a much more detailed snapshot of their targets than typical multispectral sensors, and this higher data dimensionality is critical for detecting subtle variations in vegetation health.

The MRCA coordinated ground data collection efforts of Newhall Pass oaks, which was shared with us in a comma-separated values (CSV) format. Over the months of July through September 2024, TreePeople conservation crews documented trees within 100 feet of roads and trails on MRCA lands. Using the ArcGIS Survey123 application on tablets, they reported point coordinates, tree species, crown ratings, infestation classifications, beetle hole counts, and other observations for 815 single- and multi-stemmed oak trees (1091 stem tags in total). In addition to this more extensive survey, the MRCA resurveyed representative oak trees with a Trimble, allowing us to rely on data points with greater locational accuracy for our classification. The MRCA also partnered with California State University, Northridge to obtain 2.08 megapixel multispectral and Red Green Blue (RGB) imagery of the surveyed areas using a DJI P4 Multispectral Agricultural Drone.

3.1.2 Risk Assessment Map

The risk assessment map required relevant geospatial data across Los Angeles (LA) and Ventura counties to model (1) known GSOB infestations, (2) the movement and storage of wood sources that could spread GSOB, and (3) the environmental factors that could increase oaks' susceptibility to GSOB infestation. For the known GSOB infestations, we obtained locations of infested trees throughout Southern California recorded on the Calinvasives database, then we appended the MRCA ground survey's infested tree points for a more complete record (Calinvasives, n.d.).

For the second category of inputs, we selected firewood vendors to represent sources of firewood as well as campgrounds and residential building footprints as representations of firewood consumption locations. We gathered point locations of businesses likely to sell firewood from the Data Axle Reference Solutions United States Business Database with access provided through the LA County Library (Data Axle, n.d.). Within LA and Ventura Counties, we searched for North American Industry Classification System (NAICS) codes 45721013 "firewood", 45721016 "wood pellets fuel", 45721015 "Wood (tree service and landscaping)", 3219909 "Firewood manufacturers", 447110 "gas stations with convenience stores", and 444110 "Home centers". We also obtained LA and Ventura County campground point data, where infested firewood may be brought for campfires (Jacobi et al., 2011), from the LA County Data Portal, California State Geoportal, and geocoded addresses listed on the Ventura Parks website (Internal Services Department Enterprise GIS Section, County of Los Angeles, 2016; Seth Paine, 2018; Ventura County Parks, n.d.). We accessed potentially residential (i.e., non-commercial, non-industrial) building footprints, where infested firewood could be stored outside, for each county from the Los Angeles Region Imagery Acquisition Consortium and County of Ventura Data Portal (County of Los Angeles, 2014; Kaart, 2022).

For the third category of inputs, environmental susceptibility factors, we assembled spatial data that for past wildfires and land surface temperature, two variables known to weaken oaks' defenses against the GSOB (Ray et al., 2019; Kozhoridze et al., 2023). We found historical fire perimeters from CALFIRE's Fire and Resource Assessment Program, updated as of 2023 (CALFIRE, 2024). Lastly, we obtained Landsat 8 TIRS and Landsat 9 TIRS-2 Level 2 Collection 2 Tier 1 land surface temperature data (specifically, ST_B10) through the Google Earth Engine Application Programming Interface (API) over July – October 2024 to incorporate the impact of the previous year's heat into our risk assessment map (Table C2).

3.1.3 Landcover Change Analysis

We acquired Sentinel-2 Multispectral Instrument (MSI) Level-1C data through the Google Earth Engine API. MSI data has proven valuable for long-term oak forest canopy monitoring due to its wide availability, high spatial resolution (10 m), and frequent revisit period (5 days at the equator) (Grabska-Szwagrzyk & Tymińska-Czabańska, 2024). We selected the Level-1C product to fill gaps in the 2018 imagery that were missing in Google Earth Engine's Level-2A product. To observe the peak phenological period when oak trees experience environmental and beetle-related stress (Grünzweig et al., 2008; Coleman et al., 2014) and to account for years prior to known infestation, we filtered imagery for the months of May through September for each year from 2018 to 2024.

3.2 Data Processing

3.2.1 Infested Oak Classification Map

In ArcGIS Pro v3.3.0, we imported the CSV file and converted it to points. Using the study area UAV imagery, we manually adjusted iPad-collected GPS points to center over oak crowns, as GPS accuracy can range up to 5 meters. Points that could not be reliably located on an oak, as well as those on completely dead trees, were deleted. We also removed any points with comments indicating uncertainty about beetle holes. We aggregated crown ratings to account for subjectivity among observers, combining "healthy crown" with "minor dieback" and "moderate dieback" with "severe dieback". Since the association between number of beetle holes and tree health was not statistically significant, we simplified ratings to a binary classification: with beetle holes and without.

We first mosaicked AVIRIS-3 imagery tiles and clipped them to our study area extent in ENVI v6.0. Upon export, ENVI v6.0 automatically removed the "bad bands" that introduce noise due to water vapor absorption (detailed in the data's provided header file). We then applied a BRDF (Bidirectional Reflectance Distribution Function) correction to account for variations in illumination, sensor viewing geometry, and topography between flightlines.

In ArcGIS Pro v3.3.0, we aligned the two-pixel offset between the AVIRIS-3 and UAV imagery by applying the Georeferencing tool to the AVIRIS-3 data. Then, we isolated oak pixels to reduce confusion between classes, optimizing feature relevance, and enabling the classifier to better recognize beetle infestation spectral signatures within a single vegetation type. To exclude built-up areas, such as roads and houses, we calculated a Normalized Difference Vegetation Index (NDVI) for the study area using narrowly defined spectral bands in the near-infrared (NIR, 'Band_50') and red (RED, 'Band_27') containing surface reflectance values (Equation 1; Kriegler et al., 1969). We then extracted AVIRIS imagery pixels for vegetated areas where NDVI exceeded 0.3, a threshold determined by manually examining cell values of developed areas.

$$NDVI = \frac{NIR-RED}{NIR+RED} \quad (1)$$

Visual inspection of aerial UAV imagery, along with guidance from MRCA oak point data, provided the basis for creating training samples. Initially, we classified the data into four classes: soil, dead vegetation, other vegetation, and oaks, and then reclassified into two groups, oak and non-oak. We tested multiple classifiers using an independent dataset in R Studio 2024.9.0, including K-Nearest Neighbors (KNN), Random Tree (RT), and SVM. All classifiers showed comparable accuracy across performance metrics, including K-Fold Cross-Validation, Area Under the Receiver Operating Characteristic Curve (AUC-ROC), and McNemar's Test (Table 1). We selected the Random Tree classifier with 5 neighbors and a maximum of 1,000 samples per class based on visual alignment with UAV imagery to use for the oak/non-oak binary classification.

Table 1

Classifier Accuracy for Test Classifications of Healthy versus Unhealthy Oak Tree Canopies Compared to Reference Data where Accuracy describes the model's ability to make predictions after being trained & tested on the entire dataset and K-Fold Cross Validation describes the model's ability to make predictions after being trained & tested on iteratively smaller subsets of the entire set

Classifier	Accuracy	Kappa	AUC	K-Fold Cross-Validation
KNN (1 neighbor)	96.3%	0.9	0.95	96%
KNN (5 neighbors)	97.2%	0.9	0.97	96%
RT	100%	1.0	1.0	100%
SVM	100%	1.0	1.0	100%

We then used ENVI 6.0's Principal Component Analysis tool to reduce the dimensionality of the AVIRIS oak imagery to 20 principal components for the purposes of segmentation. We passed the output into ENVI's image segmentation algorithm, which split the oak classification raster into multiple smaller groups with spectrally similar pixels, which we called "canopies". The canopy delineations guided the extraction of the hyperspectral AVIRIS data to a CSV file, which contained averaged hyperspectral values for each canopy. We additionally independently aggregated ground-truth points to train the both the RT and SVM models (as they both had a high level of initial accuracy) for the Infested Oak Classification, associating them with the spectra of each pixel in the canopy under which they fell.

3.2.2 Risk Assessment Map

We generated 30-m Euclidian distance raster layers in ArcGIS Pro v3.3.0 from firewood vendors, campgrounds, residential building footprints, and known infestation locations. For the historical fire perimeters, we created a raster containing the date of the most recent fire. For the land surface temperature data ('ST_B10'), we independently cloud-masked and removed quality flags from the Landsat 8 and Landsat 9 collections within Google Earth Engine, removing pixels coded as clouds in 'QA_PIXEL' and pixels coded as saturated or high reflectance with 'QA_RADSAT'. Additionally, we masked pixels outside the valid surface temperature and surface reflectance ranges as stipulated by the United States Geological Survey. Lastly, we applied scaling factors using a pre-existing function (located on the GEE Data Catalog Code Editor section of both Landsat 8 and Landsat 9's pages) to convert the raw data into physical quantities. We then fused the two datasets together to increase the temporal resolution and generated a median composite of land surface temperatures over July through October 2024, the four hottest months experienced by LA County that year. We removed built surfaces from this thermal layer with an NDVI mask generated using the same median composite method over the same four months. The red and NIR inputs came from Landsat 8 and 9's 'SR_B4' and 'SR_B5' bands respectively. Through visual inspection, we manually determined a threshold of 0.15 or greater to consider thermal data for vegetation across oak woodlands, mixed chaparral habitats, and urban communities encompassing both counties.

3.2.3 Landcover Change Analysis

First, we first filtered the Level-1C scenes with a cloudy pixel percentage less than 10% and clipped them by the study area extent. We then used the Google Earth Engine "SIAC" module, developed as part of Yin et al. (2022)'s Sensor Invariant Approach to Atmospheric Correction, to convert the Level-1C Top-of-Atmosphere reflectance to surface (Bottom-of-Atmosphere) reflectance. From there, we utilized bands 'B4' and 'B8' as the RED and NIR inputs, respectively, to create monthly NDVI mean composites in Google Earth Engine and exported an NDVI raster for May through September for each year over 2018-2024. We selected NDVI as our landcover change metric as it both serves as an indicator of vegetation health and uses readily accessible multispectral bands (Grabska-Szwagrzyk & Tymińska-Czabańska, 2024)

We further processed the NDVI raster layers using R v4.4.1 within RStudio v2024.09.0 Build 375. First, we stacked the NDVI rasters chronologically using the 'raster' R package v3.6-30. Next, we used the infested oak classification (resampled from 2.9 m to 10 m using the nearest neighbor method for resolution compatibility) as a mask to create separate raster stacks for non-infested and potentially infested pixels.

3.3 Data Analysis

3.3.1 Infested Oak Classification Map

After tuning hyperparameters and testing both approaches against a sample dataset, we decided to move on with the SVM, which had slightly better overall accuracy of 76%. We validated the results with a confusion matrix, which detailed how accurately each individual class was categorized (Section 4.1.1). We used our ground-truth data to train our model to classify canopies into two classes: Healthy and Infested. We then wrote a script to export the canopy classification to a raster in order to visualize the predicted class distributions over the entire study area.

3.3.2 Risk Assessment Map

We used the six previously described layers (distance to firewood vendors, campgrounds, residential buildings, known GSOB infestations, historical fire perimeters and land surface temperature), in ArcGIS Pro v3.3.0 with the Suitability Modeler (available with a Spatial Analyst license). We used a criteria model weighted by multipliers. Each layer was normalized to a 0 – 10 scale with a continuous function linear transformation. The distance to firewood vendors, campgrounds, residential buildings, and known infestations were transformed so that points at 0 m distance received a score of 10, with the score then linearly decreasing with increasing distance. The transformations for distance to firewood vendors, campgrounds, and residential buildings decreased to a score of 0 at distances beyond 9.3 km. The 9.3 km cutoff was chosen because the GSOB can travel up to 9.3 km per generation, with a single generation per year (Venette et al., 2015). The transformation for distance to known infestations decreased linearly to a score of 0 at the furthest distance

within LA and Ventura Counties. The 9.3 km cutoff was not applied to known infestations because it would yield an undesirably low risk estimate by assuming there are no infested trees beyond those surveyed. The historical fire layer was transformed so that a 2023 fire received a score of 10, with the score then linearly decreasing into the past. Meanwhile, the land surface temperature layer was transformed so that the highest temperature received a score of 10, with the score linearly decreasing to a score of 1 at the lowest temperature. We ran multiple iterations of the Suitability Modeler, varying the weight of the GSOB infestation datapoints layer, as this is the only confirmed GSOB vector in our analysis. We also ran iterations leaving each component out to see the overall effect on the high-risk areas. The Suitability Modeler sums each layer after multiplying by any weights. The output raster was reclassified into 10 categories by quantile with a blue-to-red color-blind-friendly gradient.

3.3.3 Landcover Change Analysis

We applied a pixel-based linear regression approach to estimate the rate of change in NDVI per month for each 10-m pixel. First, we extracted the NDVI value pixel-by-pixel for each month's layer within the raster stack and generated an array. We then ran a simple linear regression on every pixel's array using time (in months) as the independent variable and NDVI as the dependent variable. Finally, we created a raster that only selected pixels whose slopes were statistically significant ($p<0.05$). We repeated this process for both the healthy and potentially infested raster stacks. After generating the rasters, we performed a two-sample, two-sided Kolmogorov-Smirnov test to assess differences between the two distributions. This nonparametric test was appropriate given the non-normality of the distributions and the unequal sample sizes (Section 4.1.3).

4. Results

4.1 Analysis of Results

4.1.1 Infested Oak Classification

The areas of infestation within the study region cover approximately 820 acres (24.9% of oak cover), while non-infested areas make up around 2,469 acres (75.1% of oak cover; Figure 2). Using an independent dataset, we ran an accuracy assessment, our model was able to accurately identify infested trees 74.7% of time (producer accuracy), and non-infested trees 80.2% of the time (Table 2), with an overall accuracy 76.7% The model is slightly more likely to misclassify an infested tree as non-infested tree rather than other way around.

Figure 2. A map of the infested oak extent in the Santa Clarita Valley Study Area classified by the SVM model based on AVIRIS-3 imagery

Table 2
Confusion Matrix

		Classified data		
		Infested	Non-Infested	Total
Reference data	Infested	73	26	99
	Non-Infested	16	65	81
	Total	89	91	180

Spectral Profiles (Figure 3) of the mean reflectance for infested and non-infested oaks show some key differences. In the visible green wavelength range (523-568 nm), infested trees show a slight dip in reflectance. This can likely be explained by unhealthy leaves being less green due to stress. Additionally, in the NIR, from 790-1328nm, there is a pronounced difference in the spectral reflectance of infested and non-infested trees. The infested trees only reflect about 20% to 27.5% of the NIR wavelengths, while non-infested trees reflect about 22.5-30%, which aligns with expected patterns of stressed vegetation. In contrast, the SWIR part of the spectrum only showed small differences for infested versus non-infested GSOB trees.

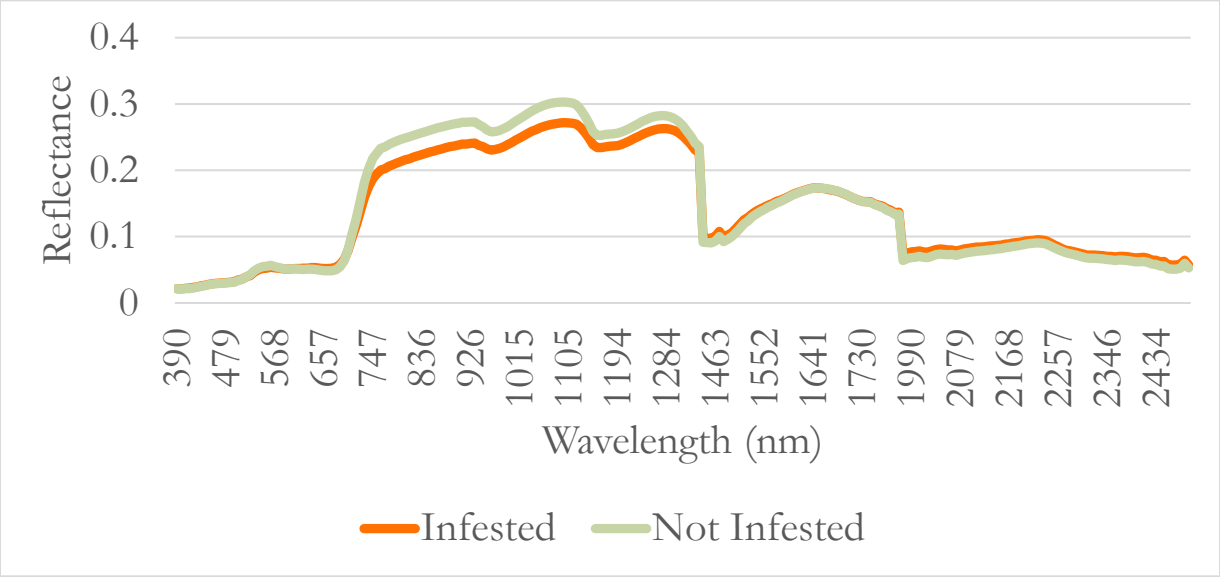

Figure 3. Spectral Profiles of GSOB infested and not infested oaks
* "Bad bands" 129-140 & 199-212 were removed from the analysis

4.1.2 Risk Assessment Map
There are multiple versions of the risk assessment map with slightly different criteria. End-users can choose which set of criteria meet their understanding of the risk factors for future GSOB infestation and find the map that most closely matches their understanding. All versions of the risk assessment map are available in our data-handoff materials. The risk map presented here (Figure 4) weights the GSOB infestation layer by 2 because it is the most guaranteed source of GSOB risk. Past fires, 2024 land surface temperature, and firewood sources (including residential buildings, campsites, and firewood vendors) were weighted by 1. There is a high-risk corridor around the Santa Clarita Valley down to the north-central portion of the Santa Monica Mountains via the mountains between Simi Valley and the San Fernando Valley. The GSOB has been observed as far south as Chatsworth in the San Fernando Valley, presenting a clear threat to the north-central

portion of the Santa Monica Mountains. However, it is important to note that the other criteria also contribute to the high-risk status of the Santa Monica Mountains. In variations of the risk assessment run with slightly different parameters, this north-central portion of the Santa Monica Mountains is consistently high-risk. Also of note is the potential spread from the Santa Clarita Valley west into the Santa Susana Mountains north of Simi Valley and east into the Angeles National Forest. Finally, there is GSOB recorded in Green Valley north of the Santa Clarita Valley, near Lancaster; this has the potential to spread west into Ventura County.

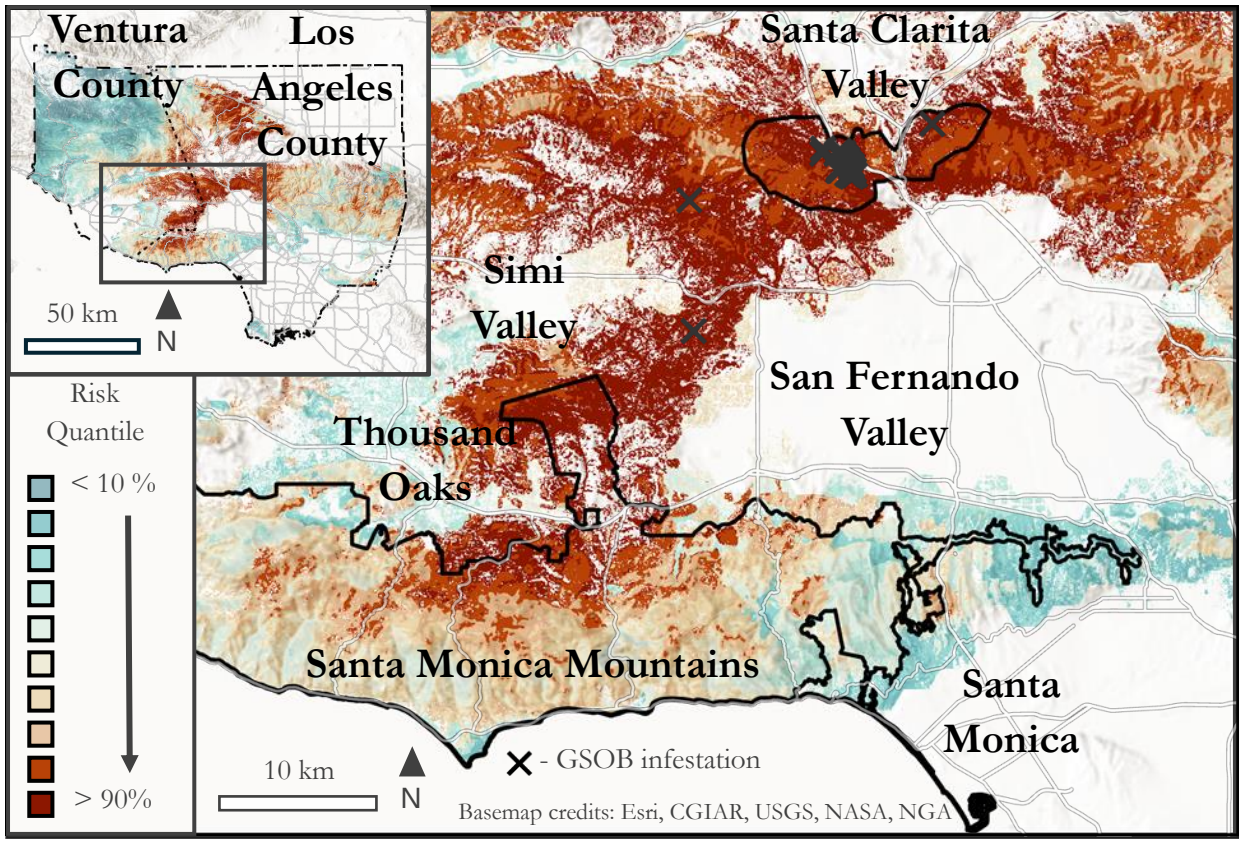

Figure 4. GSOB infestation risk assessment map of the Santa Monica Mountains and Santa Clarita Valley (black outline). Inset risk assessment map of Ventura and Los Angeles Counties. In this version of the risk assessment, the GSOB infestation points were weighted by 2, while past fires, 2024 land surface temperature, and firewood sources were weighted by 1. Red tones indicate a higher infestation risk level.

4.1.3 Landcover Change Analysis

Based on the Sentinel-2 MSI imagery, the pixel-based linear regression identified 21,728 pixels with statistically significant changes in NDVI (i.e., $p<0.05$, demonstrating a discernible trend in greenness) out of 122,946 total non-infested pixels (17.7%) and 5,027 significant pixels out of 26,488 total potentially infested (19.0%) pixels. The significant non-infested change in NDVI values ranged from -0.01347 to 0.01189 with a mean of 0.003471 and a median of 0.003514, while the significant potentially infested change in NDVI values ranged from -0.009931 to 0.01367 with a mean of 0.003355 and a median of 0.003396 (Figure 5).

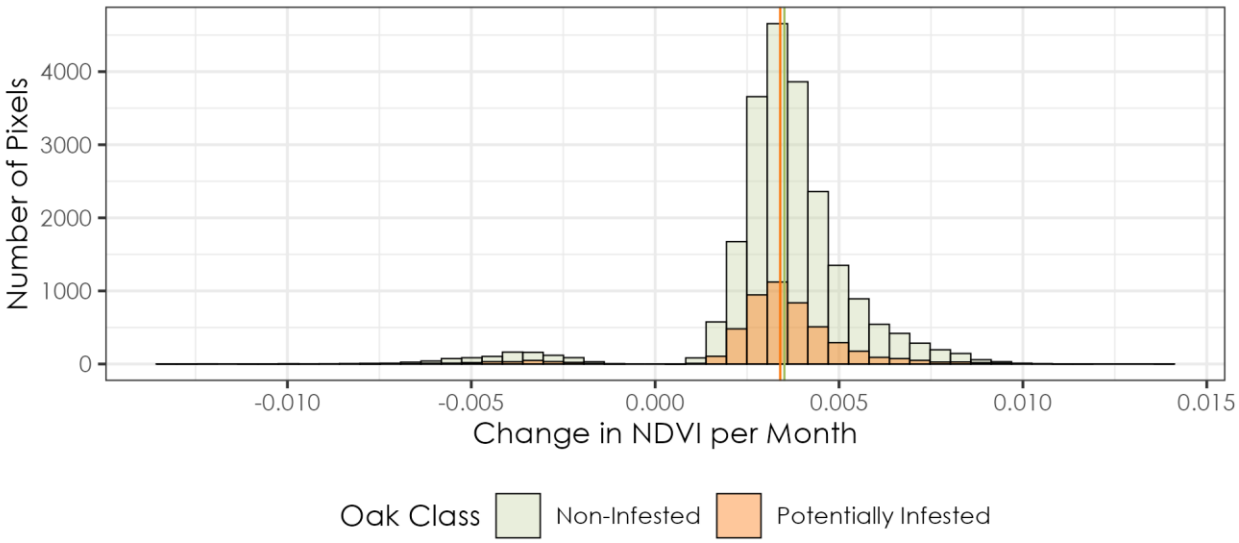

Figure 5. A histogram of statistically significant changes in NDVI separated by non-infested (green) and potentially infested (orange) classifications with vertical lines indicating respective median values.

The Kolmogorov-Smirnov test yielded a p-value of 1.973×10^{-9} and a D-statistic of 0.050396. The p-value provides strong evidence against the null hypothesis, suggesting that the two distributions are statistically different. However, both the D-statistic, which measures the maximum absolute difference between the cumulative distribution functions of the two samples, and the true mean and median difference, i.e., 0.000116 and 0.000118, are very small. In other words, although the two distributions of 10-m Sentinel-2 changes in NDVI do not share the same underlying distribution and are statistically distinct, the numerical difference between them is marginal suggesting these two distributions cannot be practically separated.

4.2 Errors & Uncertainties

4.2.1 Infested Oak Classification Map

Although the RT oak tree canopy classification had 100% accuracy, there were still places that visually did not align with observed oaks. Additionally, the orthorectified AVIRIS imagery did not perfectly align with other imagery and needed to be manually georeferenced, which could introduce error. Most tree datapoints had a five-meter accuracy, which is larger than the cell size of AVIRIS. Even though the infestation classification was object based, it is still likely that points fell on segments they did not belong to. Furthermore, oak data points were collected from only a small portion of the study area rather than being distributed across the entire region. As a result, the collected points may not fully represent the variability of oak conditions throughout the broader study area. Finally, human error in collecting oak points meant that oaks with GSOB boreholes could have been missed, and that other beetle boreholes could have been misclassified as GSOB.

Additionally, we faced some challenges with mosaicking the flightlines and the BRDF correction. Our beetle infestation map contains some areas with visible geometric boundaries, which were where the flightlines were mosaicked together. The spectral differences at the edges of the flightlines were significant enough that they affected our classification at those boundary areas. We attempted a BRDF correction to account for this, but while this significantly improved the oak classification map, the infestation map was not improved by this correction and had significant striping. Regardless, in the flightlines where we had training data, we are highly confident in our model.

4.2.2 Risk Assessment Map

The primary limitation of the risk assessment maps is that we could not quantitatively assess the importance of each criteria to inform our model weighting. If the GSOB infestation datapoints were more spatially

distributed across LA and Ventura Counties, we could have statistically tested the importance of each normalized criteria. Lacking this information, criteria normalization and weighting had to be selected according to available literature, and otherwise according to judgement. Thus, there are a variety of maps with different criteria that users can select based on their understanding of appropriate criteria weighting.

There are additional limitations for each criteria. However, the risk maps that exclude each criteria help to reveal the effect of each criteria on the model, and thus how much each criteria's limitations could affect the overall result. For the GSOB infestation, datapoints were drawn from the Calinvasives database and the MRCA's ground survey. These databases only include recorded GSOB infestations, but the full extent of GSOB infestations is likely greater. For the campsites, data points were not filtered for presence of firepits, and we also may have missed picnic areas with fire rings where people could bring infested wood. For the potential firewood vendors, companies were searched for according to NAICS codes, then the list was manually reviewed. There are certainly companies in the list that do not actually sell firewood, and many of the actual firewood vendors kiln-dry wood, which kills any beetles. This information was not captured in the firewood vendors data. Finally, residential buildings were filtered using zoning information, but many buildings, such as multi-story apartments, were included that are unlikely to store firewood. For the past fire layer, fires range in date from 1878 to 2023. There is likely a time frame after which there is little or no effect of a previous fire on risk of GSOB infestation, but due to a lack of literature on the matter, we left the normalization as linear. For the land surface temperature data, it is unclear how the land surface temperature affects tree stress compared to air temperature. We assumed that land surface and air temperature would be correlated.

4.2.3 Landcover Change Analysis

Sentinel-2's 10-m resolution both prevented analysis at the tree-scale and required resampling of the 2.9-m resolution potentially infested oak classification mask for comparisons with the Sentinel-2 imagery. We resampled the AVIRIS raster using the nearest neighbor method, which creates a 10-meter pixel grid and assigns each new pixel the value of the closest original pixel, preserving the original pixel's value without interpolation. Consequently, a single potentially infested 2.9-meter pixel could be resampled as a 10-meter pixel, inflating the infested pixel area by a maximum factor of 10.89, or it could be misclassified as non-infested (Figure B1). We observed a weak negative correlation (Spearman's correlation coefficient -0.0486) between the number of potentially infested 2.9-meter pixels within a 10-meter pixel and the NDVI slope magnitude, suggesting that resampling may remove spatial clustering effects. This resampling process diminishes the spatial variability and texture present in the original potentially infested oak classification at the 2.9-m resolution, masking subtle patterns in the data.

Moreover, seasonal oak phenology, characterized by green-up in the spring and senescence in the summer, produced similar NDVI trends for both non-infested and potentially infested areas between May and September (Figure B2). This overlap, combined with an increase in NDVI from September to May, made it difficult to isolate GSOB infestation signals from the natural phenological cycle. In comparing the spectral profiles of non-infested and potentially infested trees, differences were negligible in the visible light region, and since NDVI relies on red band reflectance, it resulted in similar trends for both oak tree health groups.

5. Conclusions

5.1 Interpretation of Results

5.1.1 Infested Oak Classification Map

The AVIRIS-3 based infested oak classification map showed high accuracy in identifying both infested and non-infested oak (Table 2). Furthermore, Figure 3 showed a clear and observable difference in the spectral signature between infested and non-infested oak. Based on these results, it can be said that AVIRIS-3 data when available can be used as a tool for further identification of GSOB infested trees.

5.1.2 Risk Assessment Map

Multiple versions of the risk assessment map show similar trends, with high-risk areas in the north-central area of the Santa Monica Mountains, around the Santa Clarita Valley, in the Green Valley area near Lancaster, and hot spots spread throughout the Angeles National Forest and the Santa Susana Mountains. Partners can view the map with the criteria and weighting that they believe to be most accurate to determine specific high-risk zones to target. Additionally, the input data, campsites, potential firewood vendors, and residential buildings, can help targeted outreach to reduce the likelihood of infested firewood GSOB spread. The MRCA and RCDSMM can hopefully convey these risk assessment maps to potential funding entities to help convey the seriousness of the issue.

5.1.3 Landcover Change Analysis

Given the significant overlap in the NDVI change value ranges for both non-infested and potentially infested pixels, we conclude that the tested 10-meter Sentinel-2 MSI-based NDVI regression method did not appear to show changes in oak woodland health related to GSOB infestations, especially within the context of oak phenological cycles. While the 10-m NDVI changes can track vegetation greenness trends over time and potentially highlight weakened stands to the MRCA, they did not in this case apparently show the infestation status of individual oak woodland pixels. Future analyses could address these limitations by utilizing data products with more NIR bands, where spectral differences between classes were more pronounced, or by incorporating additional plant health metrics beyond those related to greenness. Use of other spectral indices may enable better discrimination between infested and non-infested GSOB trees.

5.2 Feasibility & Partner Implementation

Ultimately, we demonstrated that Earth observations, particularly high-resolution AVIRIS-3 hyperspectral imagery, can play a crucial role in detecting potentially infested oaks, reducing reliance on labor-intensive ground surveys, and informing strategies for mitigating the spread of GSOB. We also highlighted the value of integrating vector datasets and remotely sensed thermal data into a GIS-based risk assessment to identify areas at risk for further spread within the MRCA and RCDSMM jurisdictions. This approach allows the MRCA and RCDSMM to prioritize future surveys and community education outreach campaigns in high-risk regions, particularly along the corridor between the Santa Clarita Valley and the Santa Monica Mountains. Additionally, we showed the limitations of using Sentinel-2 10-meter resolution NDVI trends to monitor oak woodland health in response to GSOB infestations, as the analysis did not yield statistically significant differences between the two groups. While the methods used in this study are reproducible, they may require additional computing resources to handle large file sizes and access ENVI software. Furthermore, AVIRIS's lack of regular revisiting campaigns limits the ability to update infestation extent classifications on a frequent basis. Overall, we view our project as a valuable first step in integrating Earth observations with GSOB-related oak woodland management by informing targeted conservation efforts for the MRCA and the RCDSMM.

6. Acknowledgments

We are grateful to Matthew Ribarich (MRCA) for coordinating ground truth data collection and hosting us during a field trip to the study area, and Rosi Dagit (RCDSMM) for her excitement to share knowledge and provide valuable additional points of contact throughout the project. Our science advisors—Dr. Daniel Jensen, Dr. Latha Baskaran, Dr. Zoe Pierrat, and Benjamin Holt—provided crucial research support throughout the term. We also extend our gratitude to our Center Lead, Michael Pazmino, for his support throughout our DEVELOP experience, and to our Project Coordination Fellow, Marisa Smedsrud, for her thoughtful feedback, both of whom significantly strengthened our project.

Any opinions, findings, and conclusions or recommendations expressed in this material are those of the author(s) and do not necessarily reflect the views of the National Aeronautics and Space Administration.

This material is based upon work supported by NASA through contract 80LARC23FA024.

7. Glossary

AVIRIS-3 – Airborne Visible and Infrared Imaging Spectrometer-3.
Crown rating – A classification system used to assess the health and condition of a tree's canopy.
Earth observations – Data collected from satellites and sensors to monitor the Earth's physical, chemical, and biological systems over time and space.
Euclidean distance – A measure of the straight-line distance between two points in a multi-dimensional space, commonly used in spatial analysis.
GSOB – Goldspotted Oak Borer (*Agrilus auroguttatus*).
Hyperspectral imagery – Remote sensing imagery that captures data across many more wavelengths than multispectral imagery, allowing for detailed analysis of pixels based on their spectral signatures.
Keystone species – A species essential to maintaining the structure and biodiversity of an ecosystem.
Kolmogorov-Smirnov Test (Two-Sample) – A statistical test used to compare two samples to test if they come from the same distribution.
Landsat 8 OLI & Landsat 9 OLI-2 – Operational Land Imager (Landsat 8) and OLI-2 (Landsat 9).
Landsat 8 TIRS & Landsat 9 TIRS-2 – Thermal Infrared Sensor (Landsat 8) and TIRS-2 (Landsat 9).
Linear regression – A statistical method used to model the relationship between a dependent variable and an independent variable by fitting a linear equation to observed data.
Multispectral imagery – Remote sensing imagery that captures data across a limited number of spectral bands, typically including visible and infrared wavelengths.
NIR – Near Infrared; a part of the electromagnetic spectrum just beyond the visible light range (780 nm – 2500 nm)
NDVI – Normalized Difference Vegetation Index; a remote sensing index that uses red and near-infrared bands to assess vegetation health and greenness.
Phenology – The study of cyclical events in organisms (i.e., trees) and their timing in response to environmental factors like temperature and precipitation.
Performance metrics – Statistical methods used to evaluate the performance of machine learning models. Common metrics include Area Under the Receiver Operating Characteristic Curve (AUC-ROC) (, K-Nearest Neighbors (KNN), K-Fold Cross-Validation, and McNemar's Test.
Principal Components Analysis (PCA) – A statistical technique that reduces data dimensionality by transforming it into components that retain the most significant variance.
Random Forest (RF) – A machine learning algorithm that generates multiple decision trees from random subsets of the data and aggregates their predictions. Also known as Random Tree (RT).
Segmentation – The process of dividing an image into multiple segments or regions, based on similar spectral characteristics.
Sentinel-2 MSI – Sentinel-2 Multispectral Instrument
Support Vector Machine (SVM) – A machine learning model used for classification by finding the hyperplane that best separates different classes in feature space, with the ability to tune hyperparameters for optimization.
UAV – Unmanned Aerial Vehicle; a drone or aerial vehicle used for collecting data or imagery from the air, often employed in remote sensing and surveying.

8. References

Abdel-Rahman et.al. (2014). Detecting Sirex noctilio grey-attacked and lightning-struck pine trees using airborne hyperspectral data, random forest and support vector machines classifiers. *ISPRS Journal of Photogrammetry and Remote Sensing*, *88*, 48–59. https://doi.org/https://doi.org/10.1016/j.isprsjprs.2013.11.013

CAL FIRE. (2024). Historical Fire Perimeters (Firep23_1) [Data set]. Retrieved October 16, 2024 from https://www.fire.ca.gov/what-we-do/fire-resource-assessment-program/fire-perimeters

Calinvasives. (n.d.). Agrilus auroguttatus / Goldspotted Oak Borer / GSOB [Data set]. Calflora. Retrieved October 29, 2024 from https://www.calflora.org/entry/pathogen.html?id=pth27

Coleman, T. W., Chen, Y., Graves, A. D., Hishinuma, S. M., Grulke, N. E., Flint, M. L., & Seybold, S. J. (2014). Developing Monitoring Techniques for the Invasive Goldspotted Oak Borer (Coleoptera: Buprestidae) in California. *Environmental Entomology*, *43*(3), 729–743. https://doi.org/10.1603/EN13162

Coleman, T. W., Grulke, N. E., Daly, M., Godinez, C., Schilling, S. L., Riggan, P. J., & Seybold, S. J. (2011). Coast live oak, *Quercus agrifolia*, susceptibility and response to goldspotted oak borer, *Agrilus auroguttatus*, injury in southern California. *Forest Ecology and Management*, *261*(11), 1852–1865. https://doi.org/10.1016/j.foreco.2011.02.008

Coleman, T. W., & Seybold, S. J. (2011). Collection History and Comparison of the Interactions of the Goldspotted Oak Borer, *Agrilus auroguttatus* Schaeffer (Coleoptera: Buprestidae), with Host Oaks in Southern California and Southeastern Arizona, U.S.A. *The Coleopterists Bulletin*, *65*(2), 93–108. https://doi.org/10.1649/072.065.0224

Coleman, T. W., & Seybold, S. J. (2016). Goldspotted Oak Borer in California: Invasion History, Biology, Impact, Management, and Implications for Mediterranean Forests Worldwide. In T. D. Paine & F. Lieutier (Eds.), *Insects and Diseases of Mediterranean Forest Systems* (pp. 663–697). Springer International Publishing. https://doi.org/10.1007/978-3-319-24744-1_22

Corella, K., Smith, S., Coleman, T., & Turner, K. (2020). Goldspotted Oak Borer (No. 34; Tree Notes). California Department of Forestry and Fire Protection. https://ucanr.edu/sites/gsobinfo/files/370407.pdf

County of Los Angeles. (2014). LARIAC4 BUILDINGS 2014 (Data Updated: March 13, 2023) [Data set]. County of Los Angeles Open Data. Retrieved October 15, 2024 from https://data.lacounty.gov/datasets/lacounty::lariac4-buildings-2014/explore

Data Axle. (n.d). U.S. Businesses Database [Data set]. Reference Solutions. Retrieved October 22, 2024 from http://www.referenceusa.com/UsBusiness/Search/Custom/7fd6957c22a24044a75f0415de83cc6d

European Space Agency. (n.d). Sentinel-2: Colour-vision for Copernicus. https://www.esa.int/Applications/Observing_the_Earth/Copernicus/Sentinel-2

Fassnacht, F. E., Latifi, H., Ghosh, A., Joshi, P. K., & Koch, B. (2014). Assessing the potential of hyperspectral imagery to map bark beetle-induced tree mortality. *Remote Sensing of Environment*, *140*, 533–548. https://doi.org/10.1016/j.rse.2013.09.014

Foster, A. C., Walter, J. A., Shugart, H. H., Sibold, J., & Negron, J. (2017). Spectral evidence of early-stage spruce beetle infestation in Engelmann spruce. *Forest Ecology and Management*, *384*, 347–357. https://doi.org/10.1016/j.foreco.2016.11.004

Galvan, F. E. R., Pavlick, R., Trolley, G., Aggarwal, S., Sousa, D., Starr, C., Forrestel, E., Bolton, S., Alsina, M. D. M., Dokoozlian, N., & Gold, K. M. (2023). Scalable Early Detection of Grapevine Viral Infection with Airborne Imaging Spectroscopy. *Phytopathology*, *113*(8), 1439–1446. https://doi.org/10.1094/PHYTO-01-23-0030-R

Gao, B., Yu, L., Ren, L., Zhan, Z., & Luo, Y. (2022). Early Detection of *Dendroctonus valens* Infestation with Machine Learning Algorithms Based on Hyperspectral Reflectance. *Remote Sensing*, *14*(6), 1373. https://doi.org/10.3390/rs14061373

Grabska-Szwagrzyk, E., & Tymińska-Czabańska, L. (2024). Sentinel-2 time series: a promising tool in monitoring temperate species spring phenology. *Forestry: An International Journal of Forest Research*, *97*(2), 267–281. https://doi.org/10.1093/forestry/cpad039

Grünzweig, J. M., Carmel, Y., Riov, J., Sever, N., McCreary, D. D., & Flather, C. H. (2008). Growth, resource storage, and adaptation to drought in California and eastern Mediterranean oak seedlings. *Canadian Journal of Forest Research*, *38*(2), 331–342. https://doi.org/10.1139/X07-152

Haavik, L. J., Flint, M. L., Coleman, T. W., Venette, R. C., & Seybold, S. J. (2015). Goldspotted oak borer effects on tree health and colonization patterns at six newly-established sites. *Agricultural and Forest Entomology*, *17*(2), 146–157. https://doi.org/10.1111/afe.12090

Internal Services Department Enterprise GIS Section, County of Los Angeles. (2016). Campgrounds (Data updated: April 19, 2022) [Data set]. County of Los Angeles Open Data. Retrieved October 16, 2024 from https://data.lacounty.gov/datasets/lacounty::campgrounds/about

Kaart. (2022). Ventura County, CA Buildings [Data set]. ArcGIS. Retrieved October 16, 2024 from https://www.arcgis.com/home/item.html?id=f7ebd001c64841e2a38b86e532da08af

Kozhoridze, G., Korolyova, N., & Jakuš, R. (2023). Norway spruce susceptibility to bark beetles is associated with increased canopy surface temperature in a year prior disturbance. *Forest Ecology and Management*, *547*, 121400. https://doi.org/10.1016/j.foreco.2023.121400

Kriegler, F., Malila, W., Nalepka, R., & Richardson, W. (1969). Preprocessing transformations and their effect on multispectral recognition. Proceedings of the 6th International Symposium on Remote Sensing of Environment. Ann Arbor, MI: University of Michigan, 97-131.

Lawrence, R., & Labus, M. (2003). Early Detection of Douglas-Fir Beetle Infestation with Subcanopy Resolution Hyperspectral Imagery. Western Journal of Applied Forestry, 18(3), 202–206. https://doi.org/10.1093/wjaf/18.3.202

Los Angeles County Board of Supervisors. (2024). Defending LA County's Oak Trees from the Invasive Goldspotted Oak Borer (24-1713). https://file.lacounty.gov/SDSInter/bos/supdocs/191144.pdf

Mountains Recreation and Conservation Authority. (2024). *Mountains Recreation and Conservation Authority Proactive Response to Threat of Goldspotted Oak Boarer* [sic] *in Oak Trees on its Public Parkland* [Pres release]. https://mrca.ca.gov/press/14544/

Mountains Recreation and Conservation Authority. (n.d.) *About the MRCA*. https://mrca.ca.gov/about/

Ray, C., Cluck, D. R., Wilkerson, R. L., Siegel, R. B., White, A. M., Tarbill, G. L., Sawyer, S. C., & Howell, C. A. (2019). Patterns of woodboring beetle activity following fires and bark beetle outbreaks in montane forests of California, USA. *Fire Ecology*, *15*(1), 21. https://doi.org/10.1186/s42408-019-0040-1

Resource Conservation District of the Santa Monica Mountains. (n.d.). *About the RCDSMM*. https://www.rcdsmm.org/who-we-are/about-the-rcdsmm/

Sánchez-González, M., Gea-Izquierdo, G., Pulido, F., Acácio, V., McCreary, D., & Cañellas, I. (2015). Restoration of open oak woodlands in Mediterranean ecosystems of Western Iberia and California. In J. A. Stanturf (Ed.), *Restoration of Boreal and Temperate Forests* (2nd ed., pp. 371–399). CRC Press. https://doi.org/10.1201/b18809

Senf, C., Seidl, R., & Hostert, P. (2017). Remote sensing of forest insect disturbances: Current state and future directions. *International Journal of Applied Earth Observation and Geoinformation*, *60*, 49–60. https://doi.org/10.1016/j.jag.2017.04.004

Seth Paine. (2018). Campgrounds (Data Updated: October 15, 2024) [Data set]. California State Geoportal. Retrieved October 16, 2024 from https://gis.data.ca.gov/datasets/csparks::campgrounds/explore?location=34.226896,-118.628976,8.55

Venette, R. C., Coleman, T. W., & Seybold, S. (2015). Assessing the risks posed by goldspotted oak borer to California and beyond. *Gen. Tech. Rep. PSW-GTR-251. Berkeley, CA: U.S. Department of Agriculture, Forest Service, Pacific Southwest Research Station: 317-329*, *251*, 317–329. https://research.fs.usda.gov/treesearch/49999

Ventura County Parks. (n.d.). *Online Reservations*. Ventura Parks. https://venturaparks.org/

Yin, F., Lewis, P. E., & Gómez-Dans, J. L. (2022). Bayesian atmospheric correction over land: Sentinel-2/MSI and Landsat 8/OLI. *Geoscientific Model Development*, *15*(21), 7933–7976. https://doi.org/10.5194/gmd-15-7933-2022

9. Appendix

Appendix A: *AVIRIS-3 Spectral Information*

AVIRIS-3 Band	Wavelength (nm)	AVIRIS-3 Band	Wavelength (nm)	AVIRIS-3 Band	Wavelength (nm)	AVIRIS-3 Band	Wavelength (nm)
0	389.8	33	635	66	881	99	1127.1
1	397.2	34	642.4	67	888.4	100	1134.6
2	404.6	35	649.9	68	895.9	101	1142
3	412	36	657.3	69	903.4	102	1149.5
4	419.4	37	664.8	70	910.8	103	1157
5	426.8	38	672.2	71	918.3	104	1164.4
6	434.2	39	679.7	72	925.7	105	1171.9
7	441.6	40	687.1	73	933.2	106	1179.3
8	449	41	694.6	74	940.7	107	1186.8
9	456.5	42	702	75	948.1	108	1194.2
10	463.9	43	709.5	76	955.6	109	1201.7
11	471.3	44	716.9	77	963	110	1209.1
12	478.7	45	724.4	78	970.5	111	1216.6
13	486.2	46	731.8	79	978	112	1224.1
14	493.6	47	739.3	80	985.4	113	1231.5
15	501	48	746.7	81	992.9	114	1239
16	508.4	49	754.2	82	1000.3	115	1246.4
17	515.9	50	761.7	83	1007.8	116	1253.9
18	523.3	51	769.1	84	1015.3	117	1261.3
19	530.8	52	776.6	85	1022.7	118	1268.8
20	538.2	53	784	86	1030.2	119	1276.2
21	545.6	54	791.5	87	1037.6	120	1283.7
22	553.1	55	798.9	88	1045.1	121	1291.1
23	560.5	56	806.4	89	1052.5	122	1298.6
24	568	57	813.9	90	1060	123	1306.1
25	575.4	58	821.3	91	1067.5	124	1313.5
26	582.8	59	828.8	92	1074.9	125	1321
27	590.3	60	836.2	93	1082.4	126	1328.4
28	597.7	61	843.7	94	1089.8	127	1335.9
29	605.2	62	851.2	95	1097.3	128	1343.3
30	612.6	63	858.6	96	1104.8	141	1440.2
31	620.1	64	866.1	97	1112.2	142	1447.6
32	627.5	65	873.5	98	1119.7	143	1455.1

Table A1 cont.

AVIRIS-3 Band	Wavelength (nm)	AVIRIS-3 Band	Wavelength (nm)	AVIRIS-3 Band	Wavelength (nm)	AVIRIS-3 Band	Wavelength (nm)
144	1462.5	177	1708.1	233	2123.8	266	2368
145	1470	178	1715.5	234	2131.2	267	2375.3
146	1477.4	179	1723	235	2138.6	268	2382.7
147	1484.9	180	1730.4	236	2146	269	2390.1
148	1492.3	181	1737.8	237	2153.4	270	2397.5
149	1499.7	182	1745.3	238	2160.8	271	2404.9
150	1507.2	183	1752.7	239	2168.2	272	2412.3
151	1514.6	184	1760.1	240	2175.6	273	2419.7
152	1522.1	185	1767.6	241	2183	274	2427
153	1529.5	186	1775	242	2190.4	275	2434.4
154	1537	187	1782.4	243	2197.8	276	2441.8
155	1544.4	188	1789.8	244	2205.2	277	2449.2
156	1551.9	189	1797.3	245	2212.6	278	2456.6
157	1559.3	213	1975.5	246	2220	279	2464
158	1566.7	214	1982.9	247	2227.4	280	2471.3
159	1574.2	215	1990.3	248	2234.8	281	2478.7
160	1581.6	216	1997.7	249	2242.2	282	2486.1
161	1589.1	217	2005.2	250	2249.6	283	2493.5
162	1596.5	218	2012.6	251	2257		
163	1604	219	2020	252	2264.4		
164	1611.4	220	2027.4	253	2271.8		
165	1618.8	221	2034.8	254	2279.2		
166	1626.3	222	2042.2	255	2286.6		
167	1633.7	223	2049.7	256	2294		
168	1641.1	224	2057.1	257	2301.4		
169	1648.6	225	2064.5	258	2308.8		
170	1656	226	2071.9	259	2316.2		
171	1663.5	227	2079.3	260	2323.6		
172	1670.9	228	2086.7	261	2331		
173	1678.3	229	2094.1	262	2338.4		
174	1685.8	230	2101.5	263	2345.8		
175	1693.2	231	2108.9	264	2353.2		
176	1700.6	232	2116.4	265	2360.6		

Table A1. A table denoting AVIRIS-3 bands and their associated wavelengths.

Appendix B: *Landcover Change Analysis Results*

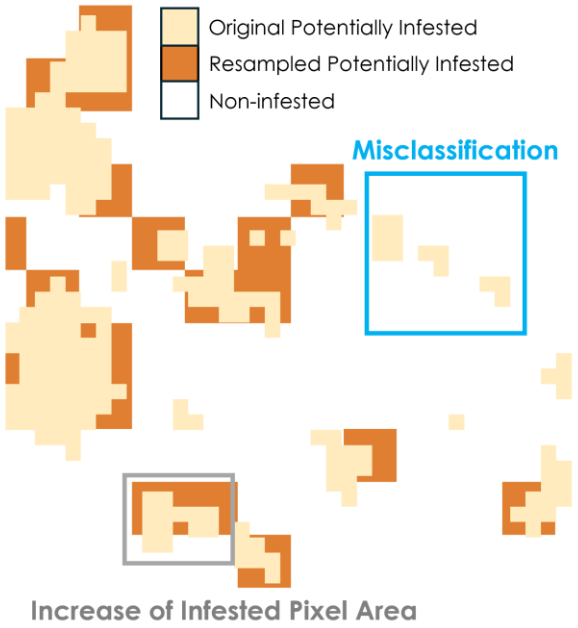

Figure B1. An illustration of two errors that may result due to nearest-neighbor resampling from 2.9-m to 10-m resolution: an inflation of the infested pixel area (gray box) or a misclassification of pixel (blue box).

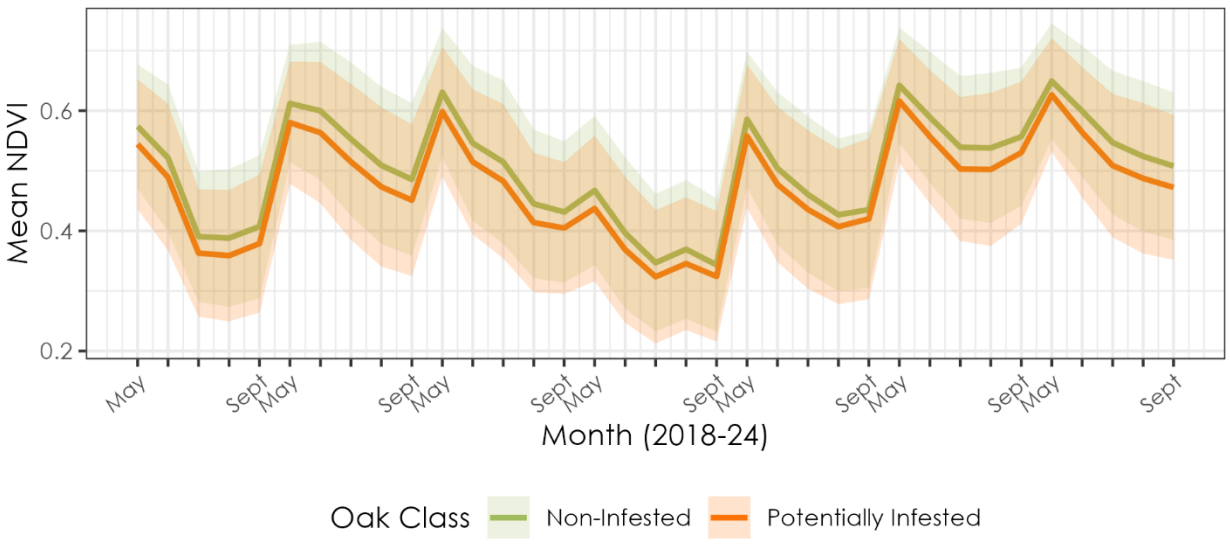

Figure B2. A time series line plot of mean NDVI separated by oak class (non-infested: green; potentially infested: orange), where shaded regions represent values within one standard deviation of the mean value.

Appendix C: Datasets Used

Table C1

Earth observations utilized

Earth Observation & Sensor	**Processing Level**	**Acquisition Platform**	**Resolution**	**Parameter**	**Timeframe**
AVIRIS-3 (B200 Aircraft)	Level 2	AVIRIS-3 Data Portal	2.9 m	Surface Reflectance	July 19, 2024
Landsat 8 OLI TIRS	Level 2, Collection 2, Tier 1	Google Earth Engine	30 m	Land Surface Temperature	July – October, 2024
Landsat 9 OLI-2 TIRS-2	Level 2, Collection 2, Tier 1	Google Earth Engine	30 m	Land Surface Temperature	July – October, 2024
Sentinel-2 MSI	Level 1C, Collection 1	Google Earth Engine	10 m	Surface Reflectance	May – September, 2018-2024

Table C2

Ancillary datasets utilized

Title	**Spatial Data Format**	**Acquisition Platform**	**Extent**	**End Product**
MRCA ground surveys	Point	Partner-collected	East Santa Clarita Valley study area	Infested Oak Tree Classification; Risk Assessment
DJI P4 Multispectral Agricultural Drone UAV imagery	Raster (RGB and multispectral imagery (2 MP))	Partner-collected	Ground survey area	Infested Oak Tree Classification
Calinvasives GSOB detections	Point	Calinvasives	California	Risk Assessment
Firewood vendors	Point	United States Business Database via Data Axle Reference Solutions	LA & Ventura Counties	Risk Assessment
LA County campgrounds	Point	LA County Data Portals	LA County	Risk Assessment
California State Parks campgrounds	Point	California State Geoportal	LA & Ventura Counties	Risk Assessment

Ventura County campgrounds	Point	Ventura Parks	Ventura County	Risk Assessment
LA County building footprints	Polygon	Los Angeles Region Imagery Acquisition Consortium	LA County	Risk Assessment
Ventura building footprints	Polygon	County of Ventura Data Portal	Ventura County	Risk Assessment
Wildfire perimeters	Polygon	CALFIRE	LA & Ventura Counties	Risk Assessment